

Experimental demonstration of Fano anti-resonance in levitated optomechanics

Chris Timberlake,^{1,*} Marko Toroš,^{1,†} David Hempston,¹ George Winstone,^{1,2} Muddassar Rashid,¹ and Hendrik Ulbricht^{1,‡}

¹*Department of Physics and Astronomy, University of Southampton, Southampton SO17 1BJ, UK*

²*School for Materials Science, Japan Advanced Institute of Science and Technology, Nomi, Ishikawa 923-1211, Japan*
(Dated: July 19, 2022)

We demonstrate a classical analogy to the Fano resonance in levitated optomechanics by applying a DC electric field. Specifically, we experimentally tune the Fano parameter by applying a DC voltage from 0 kV to 10 kV on a nearby charged needle tip. We find consistent results across negative and positive needle voltages, with the Fano line-shape feature able to exist at both higher and lower frequencies than the fundamental oscillator frequency. We can use the Fano parameter to characterize our system to be sensitive to static interactions which are ever-present. Currently, we can distinguish a static Coloumb force of $6 \pm 3 \times 10^{-16}$ N with the Fano parameter for only one second of integration time. Furthermore, we are able to extract the charge to mass ratio of the trapped nanoparticle.

I. INTRODUCTION

Resonance is of significant importance in a wide variety of fields within Physics, with the phenomena found in both classical and quantum systems. In 1961, Fano discovered that, in optics, an asymmetric line-shape arises by the interference between a discrete localized state and a continuum of states [1, 2].

Fano interference has been demonstrated in numerous quantum mechanical systems including semiconductor nanomaterials [3, 4], quantum wells [5, 6] and quantum dots [7–9], superconductors [10, 11], dielectric [12] and gold nanoparticles [13], photonic crystals [14–20], electromagnetically induced transparency (EIT) in interactions between three-level atomic systems and two laser fields [21, 22], and many other examples.

Although the Fano anti-resonance phenomena has been widely acknowledged as an effect in quantum systems, it is a general wave phenomena, meaning it can manifest itself in numerous classical systems also. Studies on the classical interpretation of the Fano resonance can be found in references [23, 24], and a theoretical comparison of the quantum and classical Fano parameter in [25]. Experimental evidence of Fano resonance has been shown for classical nanomechanical oscillators [26–30], whispering-gallery microresonators [31] and in prism-coupled square micro-pillars [32].

Levitated nanoparticles have recently emerged as very promising candidates for measuring extremely small forces. This is typically done by measuring the resonant response to a perturbation on its motion [33–35]. Levitated systems have also been used to study interactions with nearby dielectric surfaces [36, 37], and proposals have been devised to measure short range interactions like the Casimir effect [38]. Recently Hebestreit et al. proposed and demonstrated detection of static forces using free falling nanoparticles, with a sensitivity of 10 aN reported [39].

In this letter we experimentally demonstrate Fano res-

onance in levitated optomechanics. The characteristic Fano window anti-resonance is induced with a static Coulomb interaction by charging a stainless steel needle close to a charged nanoparticle in a gradient force optical trap. We show we can tune the Fano parameter by varying the voltage applied to the needle tip, and use the asymmetry in the line-shape to characterize a method of static force detection. The advantage of this method is precise force sensing irrespective of the resonant frequency. Consistent Fano parameter results were found for positive and negative applied voltages. In addition we are able to extract the charge to mass ratio of the trapped nanoparticle. We also give a phenomenological model to describe the Fano line-shape and extract a characteristic rate.

II. FANO ANTI-RESONANCE

We consider a polarizable nanoparticle trapped in an optical trap which has been described in [40]. It is convenient to define the center of the optical trap as the origin of the coordinate system: the x axis is the vertical direction pointing away from the ground, the z axis is oriented in the direction of the beam propagation away from the mirror, and the y axis is the remaining horizontal axis (see Fig. 1). To stabilize the motion at low pressure p the nanoparticle is cooled using parametric feedback cooling [41–43]. The strong cooling confines the motion of the nanoparticle to small oscillations, $\delta \mathbf{r} = (\delta x, \delta y, \delta z)^\top$, around an equilibrium position, $\mathbf{r}_{\text{eq.}} = (x_0, y_0, z_0)^\top$, which effectively decouples the translational motions. As we will discuss below, the scattering force $\mathbf{F}_s = (0, 0, F_{\text{scatt.}})^\top$ displaces the equilibrium point $\mathbf{r}_{\text{eq.}}$ away from the mirror, i.e. $x_0, y_0 \ll z_0$, which makes the z -dynamics independent of the x_0 and y_0 values. In the following we limit the discussion to the z -motion as it is experimentally the strongest signal.

The potential generated by the optical field can be

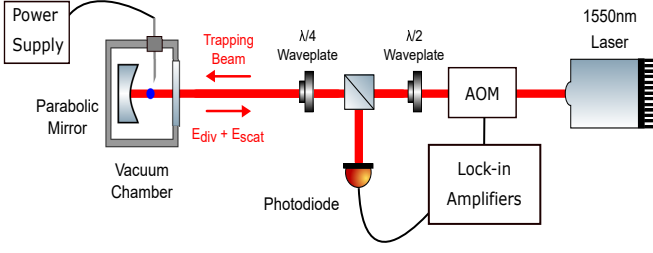


FIG. 1. Experimental setup. A silica nanoparticle is trapped, and detected, with a 1550 nm laser at the focus of a parabolic mirror. An AOM is used to modulate the laser power and cool the motion of the nanoparticle. A stainless steel needle close to the trapping site is connected to a power supply to apply a voltage which is used to manipulate the motion of a charged nanoparticle in the trap.

modeled using the following potential:

$$U_{\text{opt}}(z) = \frac{m}{2} \omega_0^2 z^2 - \eta z^4, \quad (1)$$

where m is the mass of the nanoparticle, $\omega_0^2 = \frac{2P\chi}{c\sigma_L\rho z_R^2}$ [44], P is the laser power, $\sigma_L = \pi w_0^2$ is the effective laser beam cross section area, w_0 is the mean beam waist radius, z_R is the Rayleigh length, ρ is the particle density, χ is an electric susceptibility of the particle, c is the speed of light, and η quantifies the dominant non-linearity of the trap [45].

The scattering force has only one non-zero component $F_{\text{scatt.}}(z)$ which is given in [46]. We integrate it, i.e. $\int dz' F_{\text{scatt.}}(z')$, which gives the following effective potential:

$$U_{\text{scatt}}(z) = -\frac{32\pi^3 \hbar \Gamma_s w_0^2 \tan^{-1}\left(\frac{\lambda z}{\pi w_0^2}\right)}{3\lambda^2}, \quad (2)$$

where $\Gamma_s = \frac{\sigma_R}{\sigma_L} \frac{P}{\hbar \omega_L}$ is the scattering rate, $\sigma_R = \frac{\pi^2 V^2}{\lambda^4}$ is an effective cross-section area, $\omega_L = \frac{2\pi c}{\lambda}$, and λ is the wavelength of light.

Consider now also a nearby charged needle which generates a Coulomb potential $\propto 1/|\mathbf{R} - \mathbf{r}|$, where $\mathbf{R} = (\frac{1}{\sqrt{2}}R, 0, \frac{1}{\sqrt{2}}R)$ is the position of the needle tip. For the experimental situation described in this paper only the linear contribution is relevant, specifically, expanding the Coulomb potential to and including order $\mathcal{O}(z)$ one readily finds

$$U_{\text{el}}(z) = \frac{qQz}{4\pi\epsilon_0\sqrt{2}R^2}, \quad (3)$$

where Q is the charge on the needle tip, q is the charge on the nanoparticle, and ϵ_0 is the permittivity of free space.

In addition, we apply sinusoidal modulations of the laser power P to cool the center-of-mass motion (c.m.) of the nanoparticle, namely, parametric feedback cooling. In a nutshell, one can cool a translational degree of

freedom by tracking its phase (in classical phase space) and applying a modulation at twice its harmonic frequency. Specifically, the feedback term can be obtained by making the formal replacement $P \rightarrow P(1 + \beta z p_z)$ in the equations of motion, where p_z denotes the conjugate momentum, and β is the strength of the feedback which has units of the inverse of an action, i.e. $\text{kg}^{-1}\text{m}^{-2}\text{s}$. This procedure generates the following feedback force term in the dynamics [43]:

$$f_{\text{fb}} = \beta \partial_z (U_{\text{opt}} + U_{\text{scatt}}) z p_z. \quad (4)$$

Taking into account the feedback term one obtains the following dynamics:

$$\dot{z} = \frac{z}{m}, \quad (5)$$

$$\dot{p}_z = -\partial_z U_{\text{eff}} - f_{\text{fb}} - 2\gamma_{\text{coll}} p_z + m\xi, \quad (6)$$

where the total effective potential is given by $U_{\text{eff}} = U_{\text{opt}} + U_{\text{scatt}} + U_{\text{el}}$. We have also included a damping term with coupling γ_{coll} , which is the gas collisions rate, and a noise term ξ .

We now combine Eqs. (5) and (6), using $\dot{p}_z = m\dot{z}$, and Taylor expand around the minimum position z_0 , up to and including order $\mathcal{O}(\delta z^2)$. Specifically we obtain the term $m\omega_m^2 \delta z^2/2$, where the harmonic frequency is given by

$$\omega_m = \sqrt{\omega_0^2 - \eta \frac{12z_0^2}{m} + \frac{64\pi^4 \lambda w_0^4 \hbar z_0}{3m(\pi^2 w_0^4 + \lambda^2 z_0^2)^2} \Gamma_s}. \quad (7)$$

Eq. (7) describes how the measured frequency ω_m is related to the dipole-trap harmonic frequency ω_0 , the trap non-linearity term $\propto \eta$, and the scattering force term $\propto \Gamma_s$. Here we neglect other smaller effects that could change the particle's frequency.

We are left to discuss the noise term ξ . Suppose the noise is invariant under time-translations, has zero mean, and is fully quantified by the two point correlation function $f(\tau) = \mathbb{E}[\xi(t+\tau)\xi(t)]$, where $\mathbb{E}[\cdot]$ denotes the average over different noise realizations. Exploiting the Wiener-Khinchin theorem one then readily finds the power spectral density of the z -degree of freedom: $S_{zz}(\omega) \propto \tilde{f}(\omega)/(\omega^2 \Gamma^2 + (\omega^2 - \omega_m^2)^2)$, where \tilde{f} denotes the Fourier transform of $f(\tau)$, and Γ is an effective damping rate comprising γ_{coll} as well as an additional damping contribution due to feedback term. Furthermore, assume that \tilde{f} has two distinct noise sources: one related to gas collisions $\propto \gamma_{\text{coll}}$, and one related to the Coulomb force $\propto qQ$. The term related to gas collisions, which is commonly present in optomechanical systems, leads to the usual Lorentzian power spectral density:

$$S_{\text{coll}}(\omega) \propto \frac{\gamma_{\text{coll}}}{\omega^2 \Gamma^2 + (\omega^2 - \omega_m^2)^2}. \quad (8)$$

On the other hand, the noise source $\propto qQ$ has not yet been reported in levitated optomechanics. Here we limit

the analysis to a phenomenological description of the effect, leaving a proper derivation for future work. We make the following Ansatz for the power spectral density associated to the noise perturbed Coulomb force

$$S_{\text{el}}(\omega) \propto \frac{(-f\gamma_{\text{el}}^2 + (\omega^2 - \omega_m^2))^2}{\omega^2\Gamma^2 + (\omega^2 - \omega_m^2)^2}, \quad (9)$$

where $f = e_0^2/(qQ)$ is a number, e_0 denotes the unit charge of one electron, and γ_{el} is a characteristic rate. This Ansatz has been inspired by the asymmetric Fano line-shape [1] and we will refer to f as the Fano parameter. We speculate that $S_{\text{el}}(\omega)$ could originate from a non-Markovian noise, self-induced by the motion of the nanoparticle, i.e. the motion of the nanoparticle could be perturbing the charges on the needle tip and on the particle, which would perturb back the motion of the nanoparticle on a time scale $\propto f^{-1/2}\gamma_{\text{el}}^{-1}$.

Adding all the contributions from Eqs. (8) and (9) we finally arrive at

$$S_{zz}(\omega) = A + BS_{\text{coll}}(\omega) + CS_{\text{el}}(\omega), \quad (10)$$

where A , B , and C are free parameters, i.e. fitting constants which account for the finite noise floor and normalizations. The order of magnitude of A and B can be first fixed when the charge on the needle is absent. This leaves the model with two free parameters, namely, C and γ_{el} .

III. EXPERIMENTAL SETUP

The experimental setup consists of an optical gradient force trap, which is generated by tightly focusing a 1550 nm laser with a high numerical aperture (N.A.) paraboloidal mirror [35, 42, 47]. A silica nanoparticle (density $\sim 1800 \text{ kg/m}^3$), which is trapped at the focus, has its position measured by detecting the interference generated between the Rayleigh scattered light from the particle, E_{scat} , and the divergent reference field, E_{div} , at a single photodiode (as shown in Fig. 1). The detected signal consists of information of three distinct translational frequency modes, which we will refer to as x , y and z . The z mode is in the direction of the beam propagation whereas x and y are orthogonal modes. These three modes are tracked using lock-in amplifiers, which feeds the information to an acousto-optic modulator (AOM) which applies a modulation to the laser intensity to parametrically cool the c.m. motion of the nanoparticle. A stainless steel needle, which is connected to a high voltage power supply, is placed close to the trapping region allowing us to influence the motion of the nanoparticle via the Coulomb interaction (providing the nanoparticle is charged). The fine tip of the needle results in the charge being concentrated on the needle tip, meaning the charged needle can be considered to be a point charge for

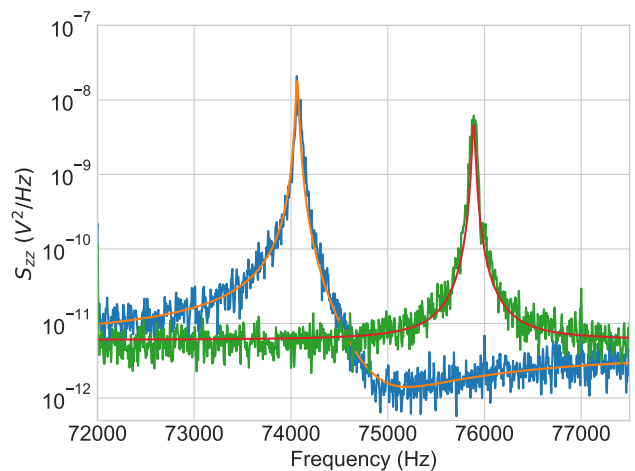


FIG. 2. The power spectral density of a levitated nanoparticle with 0 kV applied to the needle (green) and 10 kV (blue). The 0 kV peak is fitted with a standard Lorentzian distribution from Eq. (8) while the 10 kV peak is fitted with the asymmetric Fano line-shape from Eq. (10).

analytical techniques. More information on the charged needle setup can be found in [35].

IV. RESULTS

The voltage applied to the needle is swept from 0 kV to 10 kV and the effect this has on the shape of the z frequency spectrum is shown in Fig. (2). It can be seen that there is a decrease in the noise floor for a narrow bandwidth in the asymmetric line feature compared to the standard Lorentzian; this noise reduction is due to the anti-resonance suppressing the mechanical noise in this bandwidth. For an applied voltage of 10 kV the reduction in the noise floor is approximately a factor of five for a small bandwidth, known as the Fano window, around 1 kHz from the z frequency.

We have fitted Eq. (10) to data for two trapped particles in Fig. 3, exploring the regime of both the positive and the negative Fano parameter for which we find a characteristic rate, γ_{el} , of $15 \pm 2 \text{ GHz}$ (negative Fano parameter) and $23 \pm 5 \text{ GHz}$ (positive Fano parameter), respectively. We find excellent agreement at low voltages ($< 5 \text{ kV}$), with slight deviation at higher voltages ($> 5 \text{ kV}$) which might be due to additional noise sources such as the ripple voltage in the high voltage power supply.

The application of an electric field also results in a shift in the average position, as shown in reference [35]. As the laser intensity is different in the new equilibrium position there is also a corresponding shift in oscillation frequency from ω_0 to ω_m . This shift due to the varying voltage for two different particles can be seen in Fig. (4).

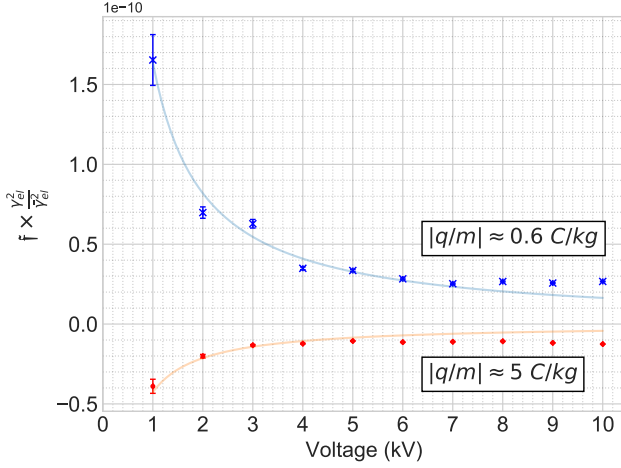


FIG. 3. The Fano parameter f for two particles as a function of applied voltage, extracted using Eq. (10). The data was taken at a vacuum pressure of 8×10^{-5} mbar and 3×10^{-5} mbar for the blue and red data, respectively. The Fano parameter f scales with the inverse of voltage, which is in good agreement with the theory.

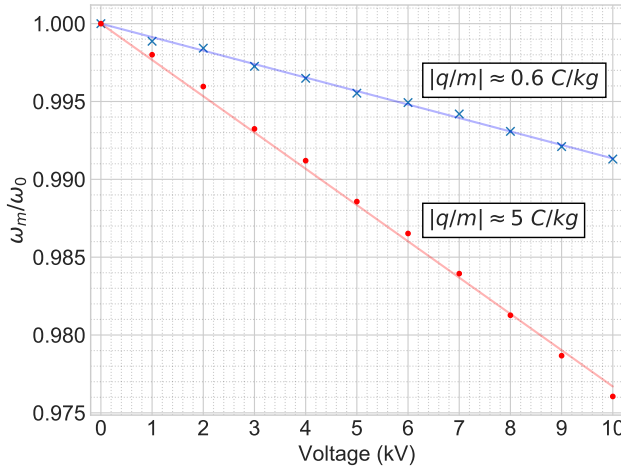


FIG. 4. Frequency shift of the z motion as a function of applied voltage to the needle, fitted using Eq. (7). The applied voltage displaces the equilibrium position of the particle's motion, which results in a change in the total potential U_{eff} the particle experiences. This results in a frequency shift which is linear with increasing voltage, to first approximation. Here two particles are plotted to show the linear response to the applied voltage. It can be seen that a larger charge to mass ratio results in a larger relative frequency shift.

V. DISCUSSION AND CONCLUSIONS

Static perturbations which cannot be "switched off" are typically hard to characterize because the oscillator experiences this static effect at all times, whereas the Fano parameter induced by such a perturbation will be present to allow characterization without "switching off",

or varying, such perturbation. For example, forces such as those induced by radiation pressure, or forces due to the Earth's gravitational attraction, could be probed using this new technique. Here we use the Coulomb interaction to characterize how sensitive our system is to such static fields.

We can use the mass of the particle and the charge on the needle tip (obtained via finite element analysis with COMSOL Multiphysics) to extract a charge on the particle; in the following we discuss results for a particle of charge $|q| = 10 \pm 5 e_0$ (charge to mass ratio $|q/m| \approx 0.6 \text{ C/kg}$). The Coulomb force induced by 1 kV applied voltage is $6 \pm 3 \times 10^{-16} \text{ N}$, however much lower forces could in principle be detected, which warrants further experimental investigation. We extract the Coulomb force by mapping the observed frequency shift in the particle motion to the expected frequency shift for a given force. This frequency shift is highly dependent on both the scattering force and the non-linearities in the gradient force potential [45]. For more sensitive characterization of static perturbation detection, further data at $< 1 \text{ kV}$ voltage on the needle is needed (or a smaller charge on the particle), and the error on the fitting will have to be small enough to distinguish between differing Fano parameters with confidence.

The needle setup can also be used for electrical state-based feedback control, such as cooling, of the motion of a charged nanoparticle [48]. A single needle can be used to drive or cool the motion of the three translational degrees of freedom, and adding a further two needles could allow precise three dimensional control. Currently, we do feedback control by modulating the power of the trapping laser at twice the frequency of our oscillator. As our trapping laser is also our detection laser, this results in the feedback signal being encoded in the particle's motion. In principle, the needle setup is advantageous as it allow us to implement linear feedback at the oscillator frequency for feedback cooling, and the signal is not mixed back into the particle signal.

The experimental setup in this paper also offers new avenues for devising experiments in static DC electrical fields. Specifically, the c.m. degree of freedom of massive levitated nanoparticles could be used to probe the validity of classical electromagnetism down to the quantum mechanical regime. In particular, one could devise an experiment consisting of a quantum mechanical system in a linear potential if the optical trap is switched off for a period of time. In addition, it could be used to investigate the electromechanical coupling and possibly quantum effects related to the nanoparticle and the electric field.

In conclusion, we have experimentally demonstrated Fano anti-resonance in levitated optomechanics by introducing an electrostatic perturbation to a charged levitated nanoparticle's potential, with the ability to tune the Fano parameter by varying the applied voltage on

a nearby charged needle. We have experimentally extracted the charge to mass ratio of trapped nanoparticles. Furthermore, we have shown that we can use the induced Fano parameter as a tool to quantify static interactions which perturb the nanoparticle's trapping potential, with a static detectable force of $6 \pm 3 \times 10^{-16}$ N reported. Although our results aren't yet comparable to the 10 aN static force sensitivity reported elsewhere [39], we note that our method can measure the force in one second, compared to averaging the results of thousands of free fall experiments. The use of the Fano parameter as a tool to measure static forces could be applied to measuring short range interactions, such as the Casimir force, and be applied for sensitive gravity detection.

VI. ACKNOWLEDGEMENTS

We would like to acknowledge A. Setter, A. Vinante and L. Ferialdi for useful discussions. We also thank G. Savage and P. Connell for their technical expertise. We would also like to thank the Leverhulme Trust [RPG-2016-046] and the EU Horizon 2020 research and innovation programme under grant agreement No 766900 [TEQ] for funding support.

* ct10g12@soton.ac.uk

† m.toros@soton.ac.uk

‡ h.ulbricht@soton.ac.uk

- [1] U. Fano, *Physical Review* **124**, 1866 (1961).
- [2] U. Fano, *Il Nuovo Cimento* **12**, 154 (1935).
- [3] C. P. Holfeld, F. Löser, M. Sudzius, K. Leo, D. M. Whitaker, and K. Köhler, *Physical Review Letters* **81**, 874 (1998).
- [4] P. Fan, Z. Yu, S. Fan, and M. L. Brongersma, *Nature Materials* **13**, 471 (2014).
- [5] J. Faist, F. Capasso, C. Sirtori, K. W. West, and L. N. Pfeiffer, *Nature* **390**, 589 (1997).
- [6] D. E. Nikonov, A. Imamoglu, and M. O. Scully, *Physical Review B* **59**, 12212 (1999).
- [7] K. Kobayashi, H. Aikawa, S. Katsumoto, and Y. Iye, *Physical Review Letters* **88**, 256806 (2002).
- [8] A. C. Johnson, C. M. Marcus, M. P. Hanson, and A. C. Gossard, *Physical Review Letters* **93**, 106803 (2004).
- [9] S. Sasaki, H. Tamura, T. Akazaki, and T. Fujisawa, *Physical Review Letters* **103**, 266806 (2009).
- [10] M. Limonov, A. Rykov, S. Tajima, and A. Yamanaka, *Physical review letters* **80**, 825 (1998).
- [11] V. G. Hadjiev, X. Zhou, T. Strohm, M. Cardona, Q. M. Lin, and C. W. Chu, *Physical Review B* **58**, 1043 (1998).
- [12] K. E. Chong, B. Hopkins, I. Staude, A. E. Miroshnichenko, J. Dominguez, M. Decker, D. N. Neshev, I. Brener, and Y. S. Kivshar, *Small* **10**, 1985 (2014).
- [13] M. I. Stockman, *Nature* **467**, 541 (2010).
- [14] A. E. Miroshnichenko, S. Flach, and Y. S. Kivshar, *Reviews of Modern Physics* **82**, 2257 (2010).
- [15] I. V. Soboleva, V. V. Moskalenko, and A. A. Fedyanin, *Physical Review Letters* **108**, 123901 (2012).
- [16] H. Yang, D. Zhao, S. Chuwongin, J.-H. Seo, W. Yang, Y. Shuai, J. Berggren, M. Hammar, Z. Ma, and W. Zhou, *Nature Photonics* **6**, 615 (2012).
- [17] M. Rybin, A. Khanikaev, M. Inoue, A. Samusev, M. Steel, G. Yushin, and M. Limonov, *Photonics and Nanostructures - Fundamentals and Applications* **8**, 86 (2010).
- [18] C. Zhou, T.-h. Tsai, D. C. Adler, H.-c. Lee, D. W. Cohen, A. Mondelblatt, Y. Wang, J. L. Connolly, and J. G. Fujimoto, *Optics Letters* **35**, 700 (2010).
- [19] P. Markoš, *Physical Review A* **92**, 043814 (2015).
- [20] M. F. Limonov, M. V. Rybin, A. N. Poddubny, and Y. S. Kivshar, *Nature Photonics* **11**, 543 (2017).
- [21] J. P. Marangos, *Journal of Modern Optics* **45**, 471 (1998).
- [22] M. Fleischhauer, A. Imamoglu, and J. P. Marangos, *Reviews of Modern Physics* **77**, 633 (2005).
- [23] Y. S. Joe, A. M. Satanin, and C. S. Kim, *Physica Scripta* **74**, 259 (2006), arXiv:0111100v1 [physics].
- [24] S. Satpathy, A. Roy, and A. Mohapatra, *European Journal of Physics* **33**, 863 (2012).
- [25] M. Iizawa, S. Kosugi, F. Koike, and Y. Azuma, *The quantum and classical Fano parameter q*, Tech. Rep. (2018) arXiv:1810.00627v1.
- [26] M. I. Tribelsky, S. Flach, A. E. Miroshnichenko, A. V. Gorbach, and Y. S. Kivshar, *Physical Review Letters* **100**, 043903 (2008).
- [27] N. Liu, L. Langguth, T. Weiss, J. Kästel, M. Fleischhauer, T. Pfau, and H. Giessen, *Nature Materials* **8**, 758 (2009).
- [28] F. Hao, Y. Sonnefraud, P. V. Dorpe, S. A. Maier, N. J. Halas, and P. Nordlander, *Nano Letters* **8**, 3983 (2008).
- [29] N. Verellen, Y. Sonnefraud, H. Sobhani, F. Hao, V. V. Moshchalkov, P. V. Dorpe, P. Nordlander, and S. A. Maier, *Nano Letters* **9**, 1663 (2009).
- [30] S. Stassi, A. Chiadò, G. Calafiore, G. Palmara, S. Cabrini, and C. Ricciardi, *Scientific Reports* **7**, 1065 (2017).
- [31] B.-B. Li, Y.-F. Xiao, C.-L. Zou, Y.-C. Liu, X.-F. Jiang, Y.-L. Chen, Y. Li, and Q. Gong, *Applied Physics Letters* **98**, 021116 (2011).
- [32] H.-T. Lee and A. W. Poon, *Optics Letters* **29**, 5 (2004).
- [33] G. Ranjit, D. P. Atherton, J. H. Stutz, M. Cunningham, and A. A. Geraci, *Physical Review A* **91**, 051805 (2015).
- [34] G. Ranjit, M. Cunningham, K. Casey, and A. A. Geraci, *Physical Review A* **93**, 053801 (2016).
- [35] D. Hempston, J. Vovrosh, M. Toroš, G. Winstone, M. Rashid, and H. Ulbricht, *Applied Physics Letters* **111**, 133111 (2017).
- [36] G. Winstone, M. Rademacher, R. Bennett, S. Buhmann, and H. Ulbricht, (2017), arXiv:1712.01426.
- [37] R. Diehl, E. Hebestreit, R. Reimann, F. Tebbenjohanns, M. Frimmer, and L. Novotny, *Physical Review A* **98**, 013851 (2018).
- [38] A. A. Geraci, S. B. Papp, and J. Kitching, *Physical Review Letters* **105**, 101101 (2010).
- [39] E. Hebestreit, M. Frimmer, R. Reimann, and L. Novotny, *Physical Review Letters* **121**, 063602 (2018).
- [40] M. Toroš, M. Rashid, and H. Ulbricht, arXiv preprint arXiv:1804.01150 (2018).
- [41] J. Gieseler, B. Deutsch, R. Quidant, and L. Novotny, *Physical review letters* **109**, 103603 (2012).

- [42] J. Vovrosh, M. Rashid, D. Hempston, J. Bateman, M. Paternostro, and H. Ulbricht, *Journal of the Optical Society of America B* **34**, 1421 (2017).
- [43] A. Setter, M. Toroš, J. F. Ralph, and H. Ulbricht, *Physical Review A* **97**, 033822 (2018).
- [44] M. Rashid, M. Toroš, and H. Ulbricht, *Quantum Measurements and Quantum Metrology* **4**, 17 (2017).
- [45] J. Gieseler, L. Novotny, and R. Quidant, *Nat Phys* **9**, 806 (2013), arXiv:1307.4684.
- [46] M. Rashid, M. Toroš, A. Setter, and H. Ulbricht, arXiv preprint arXiv:1805.08042 (2018).
- [47] M. Rashid, T. Tufarelli, J. Bateman, J. Vovrosh, D. Hempston, M. S. Kim, and H. Ulbricht, *Physical Review Letters* **117**, 1 (2016), arXiv:1607.05509.
- [48] D. Goldwater, B. A. Stickler, K. Hornberger, and J. Millen, (2018), arXiv:1802.05928.